

Multi-Objective Optimization of a Switched Reluctance Motor for Light Electric Traction Applications

Dan ILEA and Mircea M. RADULESCU

SEMLET Group

Technical University of Cluj-Napoca

Cluj-Napoca, ROMANIA

dan.ilea@mae.utcluj.ro, mircea.radulescu@mae.utcluj.ro

Frédéric GILLON and Pascal BROCHET

L2EP

Ecole Centrale de Lille

Villeneuve d'Ascq, FRANCE

frederic.gillon@ec-lille.fr, pascal.brochet@ec-lille.fr

Abstract—This paper proposes a solution for the optimization of a full-bridge three-phase inverter-fed switched reluctance motor (SRM) simultaneously accounting for the geometry of the motor as well as for its switching strategy. The optimization method proposed for this is Particle Swarm Optimization (PSO), allowing a multi-objective optimization. By means of the Permeance Network Analysis (PNA), magnetic phenomena and control scheme are both accurately modeled. The Pareto-front provides the compromise between the two objective functions imposed by the application, i.e. the average torque and torque ripple.

I. INTRODUCTION

With its various topologies and structures (radial vs. axial flux, inner vs. outer rotor, in-wheel vs. conventional drive, etc), the switched reluctance motor (SRM) presents a great adaptability to a large number of different applications. In the recent years, the SRM has become an interesting solution for light electric traction applications [1]–[3]. The main requirements on an electric motor used in such applications can be summarized as [4]:

- High power and torque density
- Wide speed range
- High efficiency over wide speed and torque range
- High reliability and robustness
- Low torque ripple and acoustic noise
- Low cost

In comparison with other types of electric traction motors (DC, induction or permanent-magnet brushless machine) the SRM has a number of advantages. The comparison made in [5] highlights the most important of them: compact and simple structure (due to the lack of magnets or windings in the rotor), extremely high speed operation and low cost.

Nevertheless the SRM has also some drawbacks that need to be corrected in order to make it competitive. The biggest of them and which is of great consequence for the traction drive is the high torque ripple induced by the doubly-salient structure of the motor.

The optimization process presented in this paper aims at reducing this torque-ripple while maintaining a reasonable average torque in order to satisfy the demands of the

application. This is done by finding the best correlation between motor geometry and switching strategy. These two components are considered simultaneously in the optimization problem.

II. FULL-BRIDGE INVERTER-FED SRM

A. Switched reluctance motor – Operating principles and mathematical model

The SRM operation is based on the variation of the stator inductance as a function of phase current and rotor position. The torque is produced by the tendency of the rotor to move to a position where the inductance of the energized stator-winding is maximized. The torque is computed using the variation of the co-energy [6] and takes into account the interaction between phases. Because of the chosen feeding solution, i.e. three-phase full-bridge inverter – which means that two phases are energized at the same time, with opposite polarities – the electromagnetic coupling between phases becomes important. The torque produced has two main components, one for each energized phase:

$$T = \frac{\partial W_c(i_1, i_2, \theta)}{\partial \theta} \Big|_{i_1, i_2 = ct} \quad (1)$$

, which may be developed further, leading to:

$$T = \frac{1}{2} \sum_{i=1}^n \varepsilon_{1i}^2 \frac{\partial \Lambda_{1i}}{\partial \theta} + \frac{1}{2} \sum_{i=1}^n \varepsilon_{2i}^2 \frac{\partial \Lambda_{2i}}{\partial \theta} \quad (2)$$

where n is the number of rotor teeth, ε_{1i} and ε_{2i} are the mmfs that appear between the stator and the rotor teeth and Λ_{1i} and Λ_{2i} are the airgap permeances.

The SRM configuration considered in this paper (Fig.1) has 6 stator teeth and 8 rotor teeth (6/8 SRM).

Because of its low computation time and reasonable accuracy levels, the Permeance Network Analysis is chosen to model the SRM [7]. This method uses the magnetic equivalent circuit of the motor (Fig.2), in order to find the permeance-current-rotor position curves and further the produced torque.

This work was supported by the Sectoral Operational Programme Human Resources Development under the POSDRU/6/1.5/S/5 ID 7676 Grant

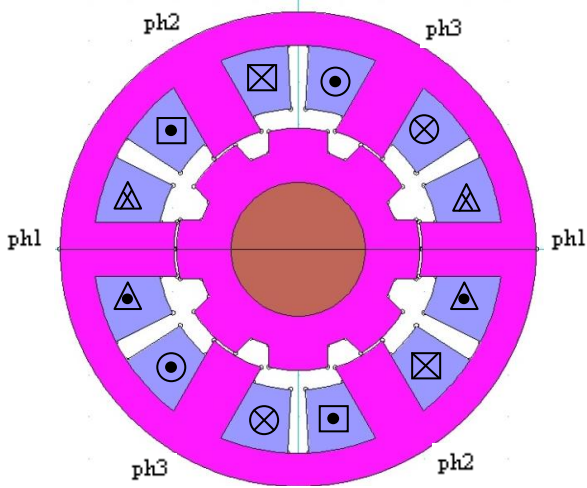


Fig.1 Geometry of the 6/8 SRM

The accuracy of the model is assured by taking into consideration all the important flux paths in the motor and the effects of mutual coupling between phases. This modular, mathematical model of the SRM is further used in the optimization step, where its reduced computation time is of great importance.

B. Control of the three-phase full-bridge inverter

Although the SRM is usually associated with a half-bridge asymmetric inverter that enables an independent phase control, for economical reasons, in the recent years a new feeding method has been developed using a standard full-

bridge inverter. The topology of the three phase full-bridge inverter along with the schematic representation of the electric circuit for the three-phase SRM is outlined in Fig. 3.

The independent feeding strategy is lost and two phases need to be energized at the same time, with opposite polarities, thus the need for a completely new feeding strategy arises.

From the different feeding methods presented in the literature for the SRM fed from a three-phase full-bridge inverter, the one presented in [8] is adopted in this paper (Fig. 4). The angle α represents the motor's stroke angle and is defined in [9] as:

$$\alpha = \frac{360^\circ}{m * N_r} = 15^\circ \quad (3)$$

where m is the phase number and N_r is the number of rotor poles.

As it can be seen, each phase is energized during $2*\alpha$ and it is turned off for α . Thus, at all moments, two phases are in conduction. It should be pointed out that only one of the two powered phases actually produces effective torque, while the other one provides only a return path for the energizing current.

However, this kind of feeding introduces new problems, e.g. phase coupling and temporary overlapping. The overlap can be avoided by correlating the geometry of the SRM with the switching strategy.

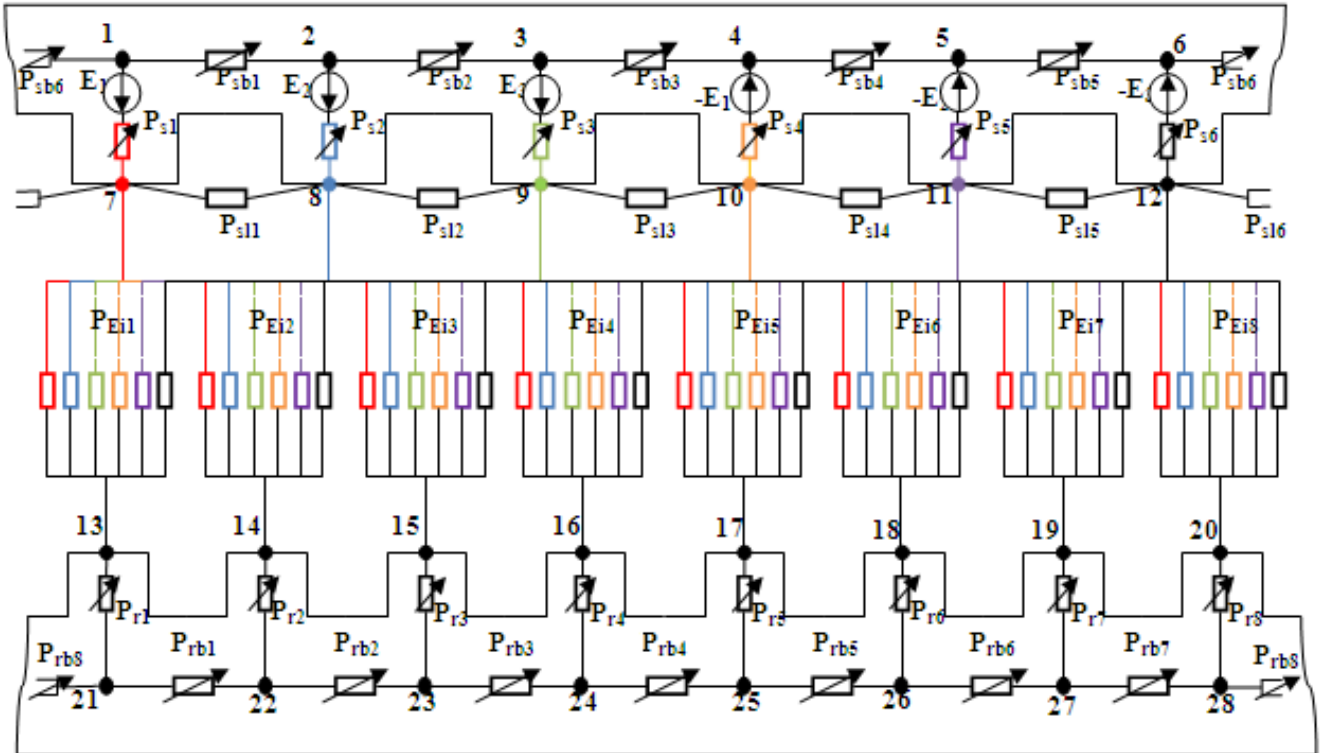


Fig.2 Linear representation of the Permeance Network for the 6/8 SRM

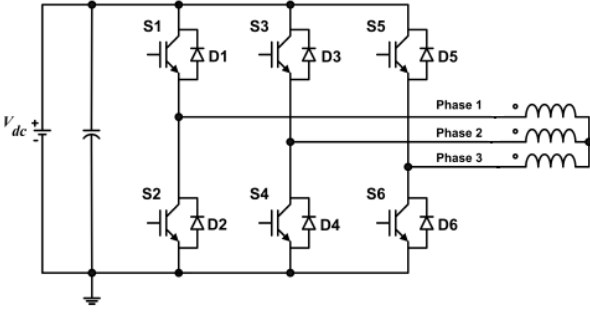


Fig.3 Schematic of a three-phase full-bridge inverter-fed SRM

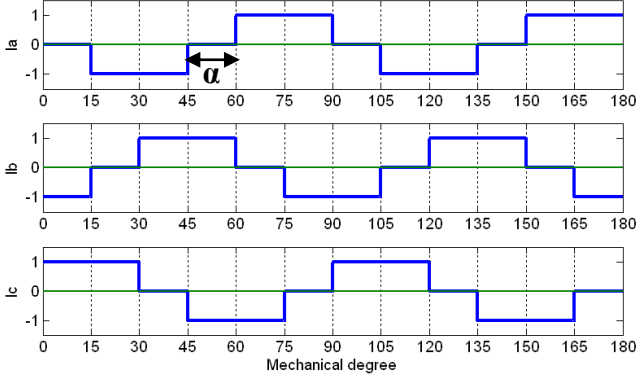


Fig.4 Switching strategy for the full-bridge inverter-fed SRM

In Fig.5 the effects of phase overlapping are shown. It can be seen that the angle between two consecutive rotor poles that pass in front of one stator phase is smaller than α . In this case, in the region where this phase should act as a returning path for the energizing current, a negative torque is produced. This torque can be limited by shifting the instant of commutation with an angle γ so that the phase will be powered only after the previous rotor pole is completely unaligned. Nonetheless, a negative torque will still be produced towards the end of the commutation period as the alignment of the current rotor pole decreases.

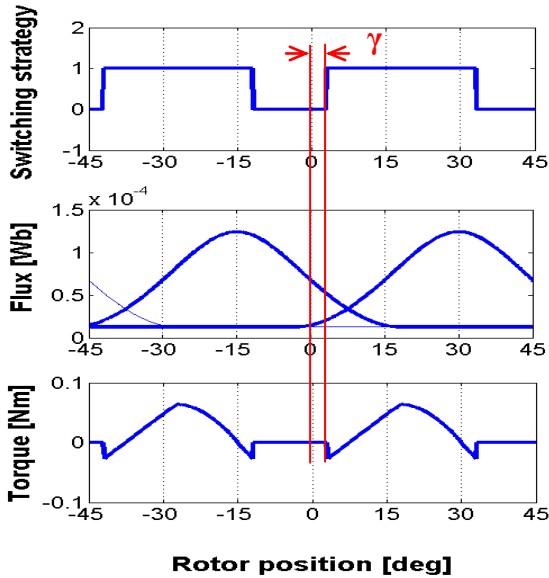


Fig. 5 Effects of phase overlap and switching strategy shifting

III. MULTI-OBJECTIVE PARTICLE SWARM OPTIMIZATION

Particle Swarm Optimization (PSO) is a population based stochastic algorithm, related to other evolutionary algorithms as Genetic Algorithm, Evolutionary Programming and Differential Evolution. It involves the experience of a number of individuals (also known as particles) which make up the population [10]. The optimization algorithm is iterative, and at each step the search is focused on the area near the best value found amongst the individuals from the previous generation, thus capitalizing on the experience of all the individuals. The PSO algorithm used in this paper, adopted from [11] can be analytically expressed as:

$$\begin{cases} \vec{v}_i \leftarrow \omega \vec{v}_{i-1} + \vec{U}(0, \phi_1) \otimes \frac{1}{\chi} (\vec{p}_i - \vec{x}_{i-1}) + \vec{U}(0, \phi_2) \otimes \chi (\vec{p}_g - \vec{x}_{i-1}) \\ \vec{x}_i \leftarrow \vec{x}_{i-1} + \vec{v}_i \end{cases} \quad (4)$$

The position \vec{x}_i of the particle is updated at each step with the particle's computed speed \vec{v}_i . This new speed takes into consideration the effect of its previous best position (\vec{p}_i) and of the best position in the entire population (\vec{p}_g). A set of two vectors of random numbers uniformly distributed in the interval $[0, \phi_i]$ - $\vec{U}(0, \phi_1)$ and $\vec{U}(0, \phi_2)$ - maintain the diversity among the individuals in the population. The inertia weight ω is introduced in order to better control the scope of the search and acts on the speed of the particle. In order to further refine the algorithm, another coefficient is introduced, called constriction coefficient χ , which controls the convergence of the particles and eliminates the need for a limit imposed on their speed.

Because the optimization problem presented in this paper has more than one optimization functions, a multi-objective approach is implemented. The algorithm used in this case is an elitist multi-objective evolutionary algorithm, based on the Pareto technique. More exactly, a slightly modified version of the solution proposed by Coello [12] is chosen, where a repository is used to store the front obtained at each step.

The initialization of the first generation of individuals is done by assigning a random value within the imposed limits for each one of the optimization variables.

The next step is the evaluation of the entire population and selection of the non-dominated individuals that will form the provisional Pareto front. An individual is non-dominated if there isn't any other individual in the population that is superior to him on all of the optimization criterions. If an individual is non-dominated it will be assigned a fitness value of zero, otherwise it will be assigned a fitness value equal to the position in the swarm of the closest individual from the front that dominates him. This is done in order to facilitate the choice of the global optimum for each individual.

$$F(m) = \begin{cases} 0 & m \geq n \quad \forall n \in P_t + \bar{P}_t \\ n & |(n > m) \wedge (dist(m, n) < dist(m, i) \forall i \in D_m) \end{cases} \quad (5)$$

where P_t and \bar{P}_t are the population and the repository, respectively, D_m is the set of individuals that dominate the individual m and \succsim is the dominance operator.

The individuals from the population that are added to the front have their position slightly modified (using a random value) in order to improve the distribution of the population over the search domain.

The best global position for each of the individuals in the population is given by the most isolated individual from the front if it dominates them or by the closest individual from the front, otherwise. This also contributes to the diversity of the final optimization front.

These steps are covered for each one of the iterations, with the new position and speed of the particles being updated according to eq. (4).

The constraints of the optimization problem are taken into consideration during the fitness evaluation of each individual. If an individual does not meet the constraints imposed, it will have its fitness value increased and therefore will not be a suitable candidate for the new front.

IV. OPTIMIZATION PROBLEM

The optimization problem takes into consideration the requirements imposed on the SRM by the traction application, i.e. value and quality of the produced torque. The two optimization objectives in this case will be torque ripple minimization and average torque maximization.

As it was previously stated, the optimization process acts simultaneously on the geometry of the motor and on its control strategy.

Because the conduction period is imposed by the number of stator and rotor poles and the use of the full bridge inverter, the only available control over the switching strategy is limited to the shifting of the commutation moments with a value γ that is adapted to the geometric structure of the SRM.

The two geometric variables that have an influence on the produced torque are the stator and rotor pole widths (w_s and w_r respectively). The limitations on w_s and w_r are imposed by the construction possibilities and the required slot area for the windings. In order to improve the modularity of the model while taking into consideration the stator and rotor diameters, the two widths are expressed using the angle at the tip of the pole, considered from the center of the axis: β_s for the stator pole and β_r for the rotor pole.

The optimization problem is formulated as:

$$SP = \min_{\substack{5^\circ < \beta_s < 40^\circ \\ 5^\circ < \beta_r < 40^\circ \\ 0^\circ < \gamma < 5^\circ}} \left(\begin{array}{l} R = \frac{T_{max} - T_{min}}{T_{rated}} * 100\% \\ T = \left| \frac{T - T_{rated}}{T_{rated}} \right| \end{array} \right) \quad (6)$$

where T_{max} , T_{min} , and T_{rated} are the maximum, minimum and rated torque values, respectively, while T and R are the two objective functions (average torque and torque ripple).

The constraints for the optimization problem are both inequalities and refer to the geometric feasibility of the proposed solutions.

$$C = \begin{cases} \beta_s - \frac{\tau_s}{2} \leq 0 \\ N_{rp} * \beta_r - \frac{3\pi}{2} \leq 0 \end{cases} \quad (7)$$

where β_s is the stator teeth angle, β_r is the rotor teeth angle, τ_s is the stator teeth pitch and N_{rp} is the number of rotor teeth.

The first condition is necessary in order to insure the slot space required for the coils, thus imposing a maximum width of the stator poles. The second condition limits the maximum width of the rotor poles and provides a minimum gap necessary in order to limit the braking torque.

The geometric dimensions for the 6/8 SRM used in the optimization process are given in Table 1.

Table 1. Geometric dimensions of the 6/8 SRM

Signification	Value	Unit
Stator core outer diameter	56.8	[mm]
Rotor core outer diameter	29	[mm]
Airgap length	0.3	[mm]
Shaft diameter	16	[mm]
Stator pole height	9.6	[mm]
Rotor pole height	2.5	[mm]
Stator back-iron	4	[mm]
Rotor back-iron	4	[mm]
Axial length	50	[mm]

In the case of the 6/8 SRM, the values of the geometric parameters used to define the optimization constraints (eq. 7) are $N_{rp} = 8$ and $\tau_s = 60^\circ$.

V. MULTI-OBJECTIVE OPTIMIZATION RESULTS

Using the algorithm described in section III, the optimization software evaluates the permeance network model of the 6/8 SRM for the two objective functions (average torque and torque ripple) and proposes a set of solutions that offer the best compromise.

The parameters used for the optimization process are presented in Table 2.

Table 2. MOPSO parameters

Number of iterations	100
Swarm size (individuals)	100
Front size	50
Inertia (ω)	0.7 (0.3 after 50 iterations)
Constriction coefficient (χ)	2 (2.5 after 50 iterations)

The graphic representation of these solutions (Pareto front) can be seen in Fig. 6, while in Table 3 the geometric variables associated with some of these solutions are presented.

As it can be seen from the presented results, the best compromise is achieved when the stator and rotor poles have similar dimensions. The average torque increases with the decrease of pole size, but in these cases the torque ripple can

exceed 100% as per eq.(6). The torque ripple is reduced in the case of wider poles. In order to obtain the best results, the switching pattern needs to be shifted with a value between 2.8° and 4° and it is specific to each geometric solution. This shift assures that the negative portion of torque produced by each phase is reduced to a minimum.

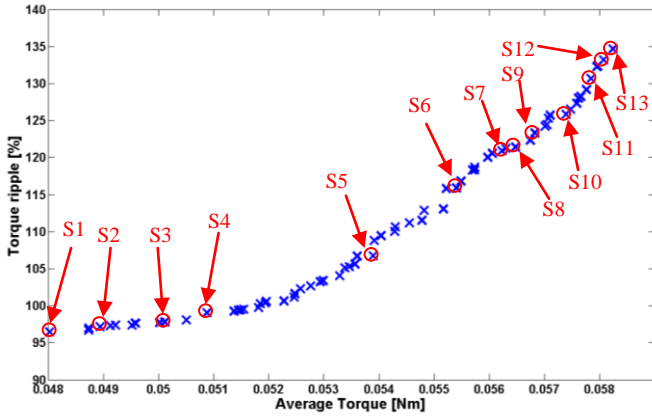


Fig. 6 Pareto front of the multi-objective PSO

Table 3. Selection of proposed optimized solutions

No.	Var. 1 (β_s) [deg]	Var. 2 (β_r) [deg]	Var. 3 (γ) [deg]	Optimization objective 1 (Average Torque) [Nm]	Optimization objective 2 (Torque ripple) [%]
1	28.65	31.1	2.88	0.0480	96.47
2	29.2	31	3.1	0.0489	97.17
3	29.88	30.4	3	0.0505	98.06
4	29.9	30.3	2.86	0.0509	99.05
5	28.56	28.78	3.1	0.054	109.5
6	28.11	27.96	3.3	0.0554	115.9
7	27.5	27.6	3.54	0.0561	120.57
8	27.3	27.5	3.42	0.0563	121.25
9	26.5	26.67	3.43	0.0571	125.72
10	26.2	26.24	3.9	0.0576	128.03
11	25.57	25.55	3.67	0.0579	132.29
12	25.57	25.6	3.67	0.058	132.37
13	25.3	25.3	3.94	0.0582	134.7

One of the optimal solutions is chosen from the current Pareto front and the torque production in this case will be analyzed. In order to validate the results obtained from the Permeance Network model of the 6/8 SRM, a Finite Element Analysis is also made using the commercial software *JMag-Studio* and the obtained torque compared.

In the case of solution no.2, β_s has a value of 29.2° and β_r is equal to 31° . The angle γ is equal to 3.1° . This gives an average torque of 0.0489 Nm and a torque ripple of 97.17 %.

The resulting dynamic torque is presented in Fig.7 along with the results obtained with FEA, for comparison. It can be seen that the accuracy of the PNA model is very good, the value and the form of the resulting torque being almost identical to that of the FEA solution.

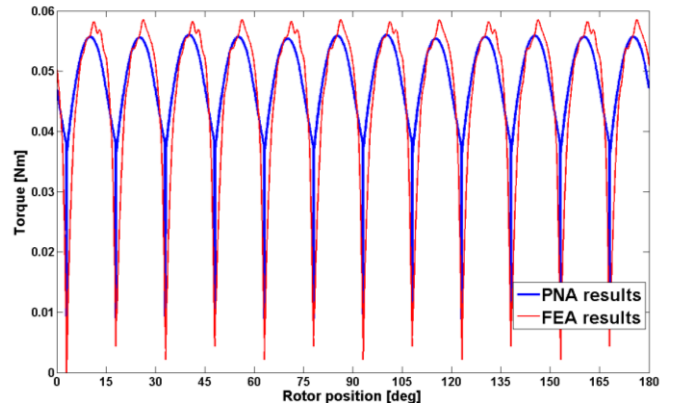


Fig. 7 Average torque for the optimized solution ($\beta_s=29.2^\circ$; $\beta_r=31^\circ$; $\gamma=3.1^\circ$) using the PNA model and FEA

Nevertheless, the computation speed for one Permeance Network model, at around 2 seconds per evaluation is far superior to that of the Finite Element simulation, which - depending on the chosen accuracy - can exceed one hour.

From this point of view, the PNA model is the only true solution for the hundreds of evaluations needed by an optimization algorithm.

VI. CONCLUSIONS AND PROSPECTS

This paper presents an optimization solution applied to the switched reluctance motor fed from a full-bridge three-phase inverter with a modified switching strategy. The objective functions are chosen in order to find the best compromise between average torque and torque ripple. This allows the improvement of an inherent issue of the SRM, thus enabling it as a suitable solution for light electric traction applications.

The modeling of the SRM is done using the Permeance Network Analysis (PNA) that offers the accuracy needed for the simulation of both the motor geometry and switching technique and also a reduced computation time requested for the optimization.

The PSO algorithm is chosen for this optimization and a modified version based on the Strength Pareto Evolutionary Algorithm (SPEA) is used to solve the multi-objective problem. The optimization variables are chosen so that the optimized solutions take into consideration both the geometry of the SRM and its switching strategy imposed by the use of the full-bridge three-phase inverter.

A dynamic, circuit-coupled Finite Element analysis of an optimized solution is performed in order to verify the validity of the PNA model.

Although the use of a full-bridge inverter can generally increase the torque ripple of the SRM, the advantages provided by this low-cost solution can sometimes be decisive. Furthermore, the careful design of the geometry of the motor in coordination with the switching strategy can reduce this ripple to a minimum and thus making the whole drive competitive as a light traction solution.

REFERENCES

- [1] M.A. Cinar, F.E. Kuyumcu, "Design and drives simulation of an in-wheel switched reluctance motor for light electric vehicle applications", *Electrical Machines&Drives Conference, IEMDC'07*, 1-4244-0742-7, Antalya, Turkey, 2007, pp.50-54
- [2] J.Lin, K.W.E. Cheng, Z. Zhang, X. Xue, "Experimental investigation of in-wheel switched reluctance motor driving system for future electric vehicles", *Power Electronics Systems and Applications, PESA'09*, 978-1-4244-3845-7, Hong-Kong, 2007, pp.1-6
- [3] A. Labak , N.C. Kar, "A novel five-phase pancake shaped switched reluctance motor for hybrid electric vehicles", *Vehicle Power and Propulsion Conference, VPPC'09*, 978-1-4244-2600-3 , Dearborn, MI, 2009, pp. 494-499
- [4] W. Xu, J. Zhu, Y. Guo, S. Wang, Y. Wang,Z. Shi, "Survey on Electrical Machines in Electrical Vehicles", *Proceedings of 2009 IEEE International Conference on Applied Superconductivity and Electromagnetic Drives*, Chengdu, China, Sept. 25-27, 2009, pp.167-170
- [5] M.Ehsani, Y. Gao, S. Gay, " Characterization of electric motor drives for traction applications", *Industrial Electronics Society IECON'03*, 0-7803-7906-3, 2-6 Nov. 2003, pp. 891-896, vol 1
- [6] H.K. Bae, " Control of switched reluctance motors considering mutual inductance", Ph.D. Thesis, VirginiaTech, Blacksburg, 2000, pp.22-24
- [7] D. Ilea, F. Gillon,P. Brochet, M.M. Radulescu, "Comparative Finite-Element and Permeance-Network Analysis for Design Optimization of Switched Reluctance Motors", *XIV International Symposium on Electromagnetic Fields in Mechatronics, Electrical and Electronic Engineering, ISEF 2009*, Arras, France, Sept. 10-12, 2009
- [8] P. Somsiri, K. Tungpimonrut, P. Aree, "Three phase full-bridge converters applied to switched reluctance motor drives with a modified switching strategy", *Proceeding of International Conference on Electrical Mahines and Systems - ICEMS 2007*, Seoul , South Korea, 8-11 October 2007
- [9] T.J.E. Miller, "Electronic Control of Switched Reluctance Motors", *Newnes Power Engineering Series*, Oxford, U.K.: Newnes, 2001
- [10] R. Poli, J. Kennedy, T. Blackwell, "Particle Swarm Optimization – An overview", *Springer Science + Business Media*, LLC 2007
- [11] M. Clerc, J. Kennedy, "The particle swarm-explosion, stability and convergence in a multidimensional complex space", *IEEE Trans. on Evolutionary Computation*, 6(1), pp. 58-73
- [12] C.A.C. Coello, G.T. Pulido and M.S. Lechuga," Handling multiple objectives with Particle Swarm Optimization ", *IEEE Transactions of Evolutionary Computation*, vol. 8, no.3, pp.256-279, June 2004